Longitudinal Automatic Carrier Landing with Explicit Nonlinear Model Predictive Controller and Improved Pigeon Inspired Optimization

Zhibing Zhang[1,3], Yang Yuan[2], Chong Zhen[1(✉)], Yimin Deng[2], and Ziqiang Li[1]

[1] Shenyang Aircraft Design & Research Institute, AVIC, Shenyang, China
zhenchong1989@163.com
[2] Beihang University, Beijing, China
[3] Nanjing University of Aeronautics and Astronautics, Nanjing, China

Abstract. In this paper, explicit model predictive controllers for velocity and altitude are designed for longitudinal control of carrier-borne aircraft, respectively. To obtain the optimal control parameters, the intelligent optimization algorithm is utilized to adjust the controller. An improved pigeon inspired optimization algorithm is proposed to obtain the optimal parameters. The superiority of the proposed method is verified by comparative simulation experiments.

Keywords: Carrier landing · Explicit nonlinear model predictive control · Improved pigeon inspired optimization

1 Introduction

Carrier-based aircraft has been playing an important role in the military field in the modern navy. It is an important cornerstone for countries to consolidate their national defense forces and enhance their international status. The autonomous carrier landing technology has attracted much more attentions as the carrier landing has certain risks in the condition of unknown deck and airwake motions [1, 2]. To make the landing aircraft control its attitude and position precisely, the automatic carrier landing system (ACLS) has been developed with various control methods [3]. The ACLS of F/A-18 is introduced in [3]. The proportional-integral-derivative (PID) controller is adopted as the basic control strategy [4]. The flight testing of the F/A-18 ACLS is described [5]. To achieve the faster tracking control ability, the H-dot ACLS is developed and proved to be disturbance resistant in many flight tests [6]. ACLS based on H-infinite technique is established for robust control in [7]. With the development of control theory, many advanced control algorithms have been proposed, such as fuzzy control, nonlinear dynamic inverse (NDI) control, and these control methods have been applied in landing control and guidance and obtained great results. SMC is utilized to develop guidance and control system in [8]. NDI and Back-stepping are applied to set up ACLS in [9, 10].

L. Yan et al. (Eds.): ICGNC 2022, LNEE 845, pp. 4116–4124, 2023.
https://doi.org/10.1007/978-981-19-6613-2_401

Explicit nonlinear model predictive control (ENMPC) uses Taylor expansion principle to obtain explicit solution of nonlinear model predictive control and avoid online optimization process [11]. In this paper, ENMPC is applied to the autonomous carrier landing to realize the fast and accurate tracking of altitude and velocity commands. Pigeon inspired optimization (PIO) algorithm is a widely used swarm intelligence algorithm due to its excellent characteristics [12–15]. However, due to its fast convergence rate, the population diversity decreases rapidly. It is difficult for the original algorithm to escape from the local optimum. To increase the population diversity, an improved pigeon inspired optimization (IPIO) with a mutation operator is proposed, which is utilized to optimize the control parameters of the ENMPC. The conclusion of the paper can be summarized as follows:

1) Longitudinal automatic carrier landing system with altitude controller and velocity controller is established with ENMPC method, and fast and accurate tracking are achieved.
2) IPIO is developed to obtain optimal controller parameters, and the advantages are demonstrated by comparison with PIO and particle swarm optimization (PSO).

2 Longitudinal Dynamic Model of Carrier-Based Aircraft

The longitudinal nonlinear dynamic model of carrier-based aircraft utilized in this paper can be expressed as follows:

$$\begin{cases} \dot{h} = V \sin \mu \\ \dot{V} = [T - (C_{D0} + C_{D\alpha}\alpha)\overline{q}S - mg \sin \mu]/m \\ \dot{\mu} = [(C_{L0} + C_{L\alpha}\alpha)\overline{q}S - mg \cos \mu]/(mV) \\ \dot{\alpha} = q - \dot{\mu} \\ \dot{q} = [C_{m0} + C_{m\alpha}\alpha + C_{mq} \cdot c/(2V) \cdot q + C_{m\delta_e}\delta_e]/I_y \end{cases} \tag{1}$$

where h represents the altitude of the aircraft, V is the velocity, μ implies the flight path angle, T is the thrust, α is the angle of attack, S is the wing area, m is the mass, g represents the gravitational acceleration, q is the pitch rate, δ_e indicates the elevator, I_y represents the moment of inertial about the pitch, C_{D0}, $C_{D\alpha}$, C_{L0}, $C_{L\alpha}$, C_{m0}, $C_{m\alpha}$, C_{mq} and $C_{m\delta_e}$ are all aerodynamic coefficients. $\overline{q}=\frac{1}{2}\rho V^2 S$, where ρ represents the air density.

3 Explicit Nonlinear Model Predictive Controller Design

In the longitudinal landing process of the carrier-based aircraft, the goal of the designed controller is to make the landing aircraft track the designed glide path accurately and keep the airspeed and angle of attack constant. The control inputs of the longitudinal model are throttle and elevator, which are utilized to control the airspeed and altitude, respectively. ENMPC method has the advantages of traditional model predictive control and does not require time-consuming online optimization process. Thus, it is applied to design the autonomous landing controller of the carrier-based aircraft.

3.1 Velocity Controller Design

Denote the output V as y_1. Due to the control input T appears in the first derivative of y_1, the relative order of the output is 1. The first derivative and the second derivative of y_1 can be expressed as follows:

$$\begin{cases} \dot{y}_1 = [T - (C_{D0} + C_{D\alpha}\alpha)\overline{q}S - mg\sin\mu]/m \\ \ddot{y}_1 = (\dot{T} - C_{D\alpha}\overline{q}S\dot{\alpha} - mg\cos\mu \cdot \dot{\mu})/m \end{cases} \tag{2}$$

where the derivative of the control input T exists in $\ddot{y}_1$.

In the process of landing, the velocity command y_{D1} is constant, and the first derivatives and second derivatives are both zero. According to design criteria of ENMPC, the following formula can be obtained:

$$(\dot{T} - C_{D\alpha}\overline{q}S\dot{\alpha} - mg\cos\mu \cdot \dot{\mu})/m = \begin{bmatrix} k_1 & k_2 \end{bmatrix} \begin{bmatrix} y_{D1} - V \\ \dot{y}_{D1} - \dot{V} \end{bmatrix} + \ddot{y}_{D1} \tag{3}$$

where k_1 and k_2 are parameters to be designed. Equation (3) can be further derived as

$$\dot{T} = m \cdot [k_1(y_{D1} - V) - k_2\dot{V} + C_{D\alpha}\overline{q}S\dot{\alpha} + mg\cos\mu \cdot \dot{\mu}] \tag{4}$$

Thus, the velocity controller has been designed.

3.2 Altitude Controller Design

Due to the small flight path angle during landing process, its sine value can be approximated by radian value. Denote the output h as y_2. Due to the control input δ_e appears in the fourth derivative of y_4, the relative order of the output is 4. Then the derivatives of y_2 can be described as follows:

$$\begin{cases} y_2 = h \\ \dot{y}_2 = \dot{h} = V\mu \\ y_2^{(2)} = V\dot{\mu} = [(C_{L0} + C_{L\alpha}\alpha)\overline{q}S - mg\cos\mu]/m \\ y_2^{(3)} = (C_{L\alpha}\overline{q}S\dot{\alpha} + mg\sin\mu \cdot \dot{\mu})/m \\ y_2^{(4)} = [C_{L\alpha}\overline{q}S(\dot{q} - \ddot{\mu}) + mg\cos\mu \cdot \dot{\mu}^2 + mg\sin\mu \cdot \ddot{\mu}]/m \\ y_2^{(5)} = [C_{L\alpha}\overline{q}S(\ddot{q} - \dddot{\mu}) - mg\sin\mu \cdot \dot{\mu}^3 + 2mg\cos\mu \cdot \dot{\mu} \cdot \ddot{\mu} + mg\cos\mu \cdot \dot{\mu} \cdot \ddot{\mu} + mg\sin\mu \cdot \dddot{\mu}]/m \end{cases} \tag{5}$$

where the control input δ_e exists in $\dot{q}$, the derivative of the control input δ_e exists in $\ddot{q}$, of which the expression is as follows:

$$\ddot{q} = \overline{q}S\overline{c} \cdot [C_{m\alpha}\dot{\alpha} + C_{mq}(c/2V)\dot{q} + C_{m\delta_e}\dot{\delta}_e]/I_y \tag{6}$$

During the landing process, the height command y_{D2} is a straight line descending uniformly with time. The first derivative $\dot{y}_{D2}$ is constant, and its second and higher derivatives are all zero. According to design criteria of ENMPC, it can be obtained that

$$y_2^{(5)} = \begin{bmatrix} k_3 & k_4 & k_5 & k_6 & k_7 \end{bmatrix} \begin{bmatrix} y_{D2} - h \\ \dot{y}_{D2} - \dot{h} \\ y_{D2}^{(2)} - h^{(2)} \\ y_{D2}^{(3)} - h^{(3)} \\ y_{D2}^{(4)} - h^{(4)} \end{bmatrix} + y_{D2}^{(5)} \tag{7}$$

where $k_i (i = 3, \cdots, 7)$ are parameters to be designed. The derivative of elevator can be obtained by solving the above equation, and the controller is designed as follows:

$$\dot{\delta}_e = \frac{\frac{\left[m\left(K_2(Y_{D2}^U - Y_2^U) + g(\dot{\mu}^3 \sin\mu - 3\dot{\mu}\ddot{\mu}\cos\mu - \dddot{\mu}\sin\mu)\right) + C_{L\alpha}\bar{q}S\ddot{\mu}\right]I_y}{C_{L\alpha}\bar{q}^2 S^2 \bar{c}} - C_{m\alpha}\dot{\alpha} - \frac{C_{mq}\bar{c}\dot{q}}{2V}}{C_{m\delta_e}} \tag{8}$$

where $K_2 = [k_3, k_4, k_5, k_6, k_7]$, $Y_{D2}^U = \left[y_{D2}, \dot{y}_{D2}, 0, 0, 0\right]^T$, and $Y_2^U = \left[h, \dot{h}, h^{(2)}, h^{(3)}, h^{(4)}\right]^T$.

To get the optimal control parameters, the intelligent optimization algorithm is utilized to adjust the controller.

4 Improved Pigeon Inspired Optimization

4.1 Original Pigeon Inspired Optimization

The PIO algorithm is proposed based on the special navigation behavior of pigeons. The algorithm consists of two stages and different operators. One is the map and compass operator and the other one is the landmark operator.

If the optimization problem is in a D dimensional space, initialize N_P pigeons with the position of $X_i = [X_{i1}, X_{i2}, \cdots, X_{iD}]$ and the velocity of $V_i = [V_{i1}, V_{i2}, \cdots, V_{iD}]$. In the map and compass operator, each individual updates its status with reference to the global optimal individual and updates its position and velocity according to the following formula:

$$V_i(k) = V_i(k-1) \cdot e^{-R_m k} + rand \cdot (X_{gbest} - X_i(k-1)) \tag{9}$$

$$X_i(k) = X_i(k-1) + V_i(k) \tag{10}$$

where k stands for the current iteration number, *rand* is a random number and set within [0,1], R_m implies the factor in the map and compass operator, and X_{gbest} is global optimal position of all individuals. When the iteration number exceeds the maximum iteration $N_{c1\max}$ in the map and compass operator, the landmark operator will be used for further search.

In the second stage, individuals with poor knowledge of the landmark would be abandoned, and the rest will fly straight to the landmark. The positions of the pigeons are updated as follows:

$$N_p(k) = \text{ceil}(\frac{N_p(k-1)}{2}) \tag{11}$$

$$X_i(k) = X_i(k-1) + rand \cdot (X_{center}(k) - X_i(k-1)) \tag{12}$$

$$X_{center}(k) = \frac{\sum_{i=1}^{N_p(k)} X_i(k) \cdot f(X_i(k))}{N_p \cdot \sum_{i=1}^{N_p(k)} f(X_i(k))} \tag{13}$$

where ceil(·) is a rounded up function, $f(\cdot)$ is the cost value function, $X_{center}(k)$ is the landmark in n iteration.

4.2 Improved Pigeon Inspired Optimization

In the exploration process of map and compass operator, X_{gbest} plays a leading role for its global optimal experience. When X_{gbest} falls into local optimal, it is difficult to escape due to all individuals are evolving towards the X_{gbest}. To improve the original PIO, an improved PIO (IPIO) based on the swarm diversity is proposed.

Firstly, all dimensions of the individual are normalized according to the following expression:

$$\widetilde{X}_{ij}(k) = \frac{X_{ij}(k) - X_{j\min}}{X_{j\max} - X_{j\min}} \tag{14}$$

where $X_{j\max}$ and $X_{j\min}$ are upper and lower boundaries of $X_{ij}(k)$.

Secondly, calculate the swarm diversity $d(k)$ as follows:

$$d(k) = \frac{\sum_{i=1}^{N_p} \sqrt{\sum_{j=1}^{D} (\widetilde{X}_{ij}(k) - \overline{X}_j(k))^2}}{N_p} \tag{15}$$

$$\overline{X}_j(k) = \frac{\sum_{i=1}^{N_p} \widetilde{X}_{ij}(k)}{N_p} \tag{16}$$

where $\overline{X}_j(k)$ is the mean value of all individuals in j_{th} dimension.

Thirdly, if the $d(k)$ is smaller than the preset threshold C_1, a mutation operator is utilized to increase swarm diversity. A random number r within [0,1] is generated. If $r > C_2$ is satisfied, the following action is performed to create new individuals:

$$\tilde{P}_i(k) = \begin{cases} P_i(k) + (X_{\max} - P_i(k)) \cdot r_1 \cdot (1 - k/N_{c1\max}) & if\ rand < 0.5 \\ P_i(k) - (X_i(k) - X_{\min}) \cdot r_2 \cdot (1 - k/N_{c1\max}) & if\ rand < 0.5 \end{cases} \tag{17}$$

where $P_i(k)$ is the personal best. If $f\left(\tilde{P}_i(k)\right) < f(P_i(k))$, the $P_i(k)$ and $X_i(k)$ are replaced by $\tilde{P}_i(k)$.

Fourthly, if k exceeds the iteration N_{c1max}, the landmark operator comes into play.

Finally, if k exceeds the maximum iteration $N_{c1max}+N_{c2max}$, the optimization process ends.

5 Simulation Results

MATLAB/Simulink is utilized as simulation software to build the carrier landing model. The parameters of the carrier-based aircraft are shown in [16, 17]. The control parameters $k_i(i = 1, \cdots, 7)$ are optimized by the proposed IPIO. The integral of time-weighted absolute value of the error (ITAE) [15] is adopted as evaluation index, given by

$$J_e = \int_0^\infty t|E(t)|dt \tag{18}$$

where $E(t)$ is altitude tracking error.

To demonstrate the superiority of the proposed IPIO, the comparison experiment is conducted with PIO and PSO. The iteration of all algorithms are 30, and the number of individuals is 20. The simulation time is set as 50 s.

The evolutionary curves of cost value are shown in Fig. 1(a), in which the cost value index of three methods ranked PIO, PSO and IPIO in descending order. It indicates that the proposed IPIO has the best search ability. The diversity curves of three methods are depicted in Fig. 2. It can be seen that the diversity of the proposed IPIO has been kept in a higher level as the iteration progresses, while the diversity of PIO decreased most rapidly. It is verified that mutation operator can improve the population diversity.

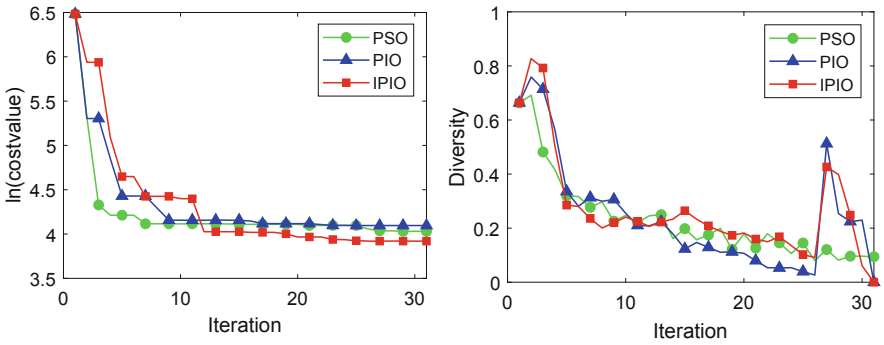

(a) Cost value (b) Diversity

Fig. 1. Evolutionary curves of three methods

The altitude tracking errors with the parameters optimized by three methods are given in Fig. 2. The tracking error optimized by IPIO has a shortest return time to zero. The time of decline to the lowest point of PSO, PIO and IPIO is 5.61 s, 5.99 s and 4.85

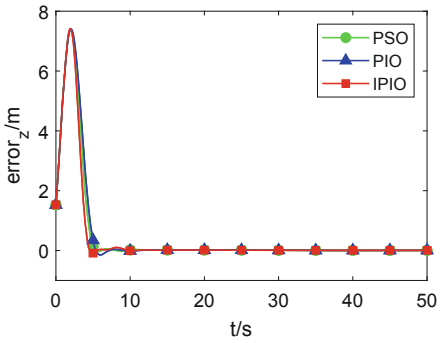

Fig. 2. Altitude tracking error

s, respectively. The time of growth to the highest point of PSO, PIO and IPIO is 2.04 s, 1.98 s and 1.95 s, respectively.

The performances of throttle output and elevator deflection are obtained and shown in Fig. 3. The fluctuation trends of the curves obtained by three methods are consistent, while there are some differences in the magnitude of fluctuation. Form Fig. 3(a), it can be seen that the thrust fluctuation of IPIO is smaller than others at about 10 s. However, the elevator fluctuation of IPIO is more violent than other methods in Fig. 3(b).

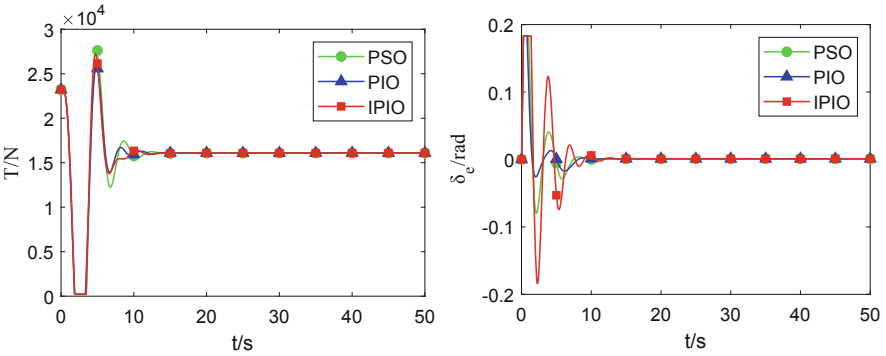

(a) Thrust (b) Elevator

Fig. 3. Throttle output and elevator deflection

Figure 4 describes the angle of attack and velocity states of the aircraft. The angle of attack first decreases, then increases, and finally stays at a constant value. It is apparent that the fluctuation of IPIO is more severe than others. The velocity of the aircraft was maintained at about 69.96 m/s, and the maximum error of IPIO is 0.64 m/s.

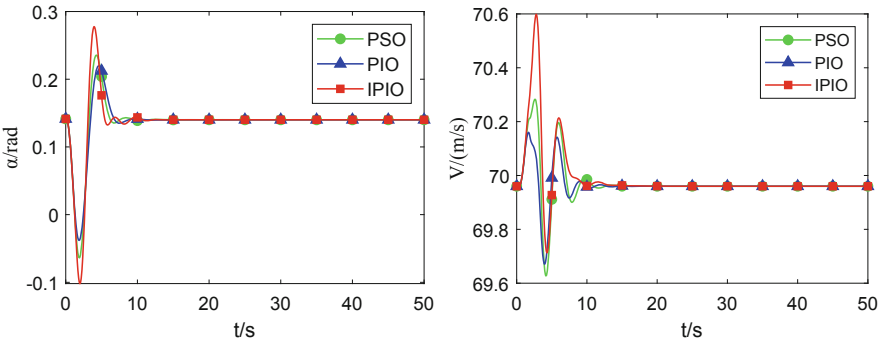

(a) Angle of attack (b) Velocity

Fig. 4. States of the aircraft

6 Conclusions

The controller of carrier-based aircraft landing has been designed in this paper. ENMPCs are designed for the longitudinal control of carrier-based aircraft. A velocity ENMPC is designed to maintain constant speed, and a height ENMPC is designed to guarantee altitude tracking. To obtain the optimal control parameters of ENMPCs, IPIO is proposed to improve the search ability. A comparison simulation experiment was conducted with PIO and PSO to verify the effectiveness of IPIO.

References

1. Zhen, Z., Yu, C., Jiang, S., Jiang, J.: Adaptive super-twisting control for automatic carrier landing of aircraft. IEEE Trans. Aerosp. Electron. Syst. **56**(2), 984–997 (2020)
2. Li, J., Duan, H.: Simplified brain storm optimization approach to control parameter optimization in F/A-18 automatic carrier landing system. Aerosp. Sci. Technol. **42**, 187–195 (2015)
3. Niewoehner, R.J., Kaminer, I.I.: Design of an autoland controller for a carrier-based F-14 aircraft using H∞ output-feedback synthesis. In: American Control Conference, Baltimore, MD, USA, pp. 2501–2505 (1994)
4. Urnes, J.M., Hess, R.K.: Development of the F/A-18A automatic carrier landing system. J. Guid. Control. Dyn. **8**(3), 289–295 (2012)
5. Prickett, A.L., Parkes, C.J.: Flight testing of the F/A-18E/F automatic carrier landing system. In: 2001 Aerospace Conference, Big Sky, MT, USA, pp. 2593–2612. IEEE (2001)
6. Urnes, J.M., Hess, R.K., Moomaw, R.F.: H-Dot automatic carrier landing system for approach control in turbulence. J. Guid. Control. Dyn. **4**(2), 177–183 (1981)
7. Subrahmanyam, M.B.: H∞ design of F/A-18A automatic carrier landing system. J. Guid. Control. Dyn. **17**(1), 187–191 (1994)
8. Lee, S., et al.: Sliding mode guidance and control for uav carrier landing. IEEE Trans. Aerosp. Electron. Syst. **55**(2), 951–966 (2018)
9. Lungu, M.: Auto-landing of fixed wing unmanned aerial vehicles using the backstepping control. ISA Trans. **95**, 194–210 (2019)
10. Lungu, M.: Backstepping and dynamic inversion combined controller for auto-landing of fixed wing UAVs. Aerospace Sci. Technol. **96**, 105526 (2019)

11. Liu, C., Chen, W., Andrews, J.: Explicit nonlinear model predictive control for autonomous helicopters. Proc. Inst. Mech. Eng. Part G J. Aerosp. Eng. **226**(9), 1171–1182 (2012)
12. Duan, H., Qiao, P.: Pigeon-inspired optimization: a new swarm intelligence optimizer for air robot path planning. Int. J. Intell. Comput. Cybern. **7**(1), 24–37 (2014)
13. Duan, H., Qiu, H.: Advancements in pigeon inspired optimization and its variants. Sci. China Inf. Sci. **62**(7), 1–10 (2019)
14. Duan, H., Wang, X.: Echo state networks with orthogonal pigeon-inspired optimization for image restoration. IEEE Trans. Neural Netw. Learn. Syst. **27**(11), 2413–2425 (2016)
15. Yuan, Y., Duan, H.: Active disturbance rejection attitude control of unmanned quadrotor via paired coevolution pigeon-inspired optimization. Aircr. Eng. Aerosp. Technol. **94**(2), 302–314 (2022)
16. Chakraborty, A., Seiler, P., Balas, G.J.: Susceptibility of f/a-18 flight controllers to the falling-leaf mode: linear analysis. J. Guid. Control. Dyn. **34**(1), 73–85 (2011)
17. Chakraborty, A., Seiler, P., Balas, G.J.: Susceptibility of F/A-18 flight controllers to the falling-leaf mode: nonlinear analysis. J. Guid. Control. Dyn. **34**(1), 57–72 (2011)